In vivo optical monitoring of transcutaneous delivery of calcium carbonate microcontainers

Elina A. Genina,[1,2] Yulia I. Svenskaya,[1] Irina Yu. Yanina,[1] Leonid E. Dolotov,[1] Nikita A. Navolokin,[3] Alexey N. Bashkatov,[1,2] Georgy S. Terentyuk,[1,3] Alla B. Bucharskaya,[3] Galina N. Maslyakova,[3] Dmitry A. Gorin,[1] Valery V. Tuchin,[1,2,4] and Gleb B. Sukhorukov[1,5]

[1]*National Research Saratov State University, 83 Astrakhanskaya Street, Saratov 410012, Russia*
[2]*National Research Tomsk State University, 36 Lenin Avenue, Tomsk 634050, Russia*
[3]*Saratov State Medical University, 112 Bolshaya Kazachaya Street, Saratov 410012, Russia*
[4]*Institute of Precision Mechanics and Control of RAS, 24 Rabochaya Street, Saratov 410028, Russia*
[5]*School of Engineering and Materials Science, Queen Mary University of London, London, E1 4NS, UK*
[*]*eagenina@yandex.ru*

Abstract: We have developed a method for delivery of biocompatible $CaCO_3$ microcontainers (4.0 ± 0.8 μm) containing Fe_3O_4 nanoparticles (14 ± 5 nm) into skin *in vivo* using fractional laser microablation (FLMA) provided by a pulsed Er:YAG laser system. Six laboratory rats have been used for the microcontainer delivery and weekly monitoring implemented using an optical coherence tomography and a standard histological analysis. The use of FLMA allowed for delivery of the microcontainers to the depth about 300 μm and creation of a depot in dermis. On the seventh day we have observed the dissolving of the microcontainers and the release of nanoparticles into dermis.

OCIS codes: (170.0170) Medical optics and biotechnology; (170.1020) Ablation of tissue; (170.0180) Microscopy; (110.4500) Optical coherence tomography; (350.4990) Particles.

References and links

1. R. L. Bronaugh and H. I. Maibach, eds., *Percutaneous Absorption. Drugs, Cosmetics, Mechanisms, Methods,* 4th ed. (Taylor & Francis Group, LLC, CRC Press, 2005).
2. G. Cevc and U. Vierl, "Nanotechnology and the transdermal route: A state of the art review and critical appraisal," J. Control. Release **141**(3), 277–299 (2010).
3. J. Lademann, F. Knorr, H. Richter, S. Jung, M. C. Meinke, E. Ruhl, U. Alexiev, M. Calderon, and A. Patzelt, "Hair follicles as a target structure for nanoparticles," J. Innov. Opt. Health Sci. **8**(4), 1530004 (2015).
4. N. Otberg, H. Richter, H. Schaefer, U. Blume-Peytavi, W. Sterry, and J. Lademann, "Variations of hair follicle size and distribution in different body sites," J. Invest. Dermatol. **122**(1), 14–19 (2004).
5. J. Lademann, H. Weigmann, C. Rickmeyer, H. Barthelmes, H. Schaefer, G. Mueller, and W. Sterry, "Penetration of titanium dioxide microparticles in a sunscreen formulation into the horny layer and the follicular orifice," Skin Pharmacol. Appl. Skin Physiol. **12**(5), 247–256 (1999).
6. Y. G. Bachhav, S. Summer, A. Heinrich, T. Bragagna, C. Böhler, and Y. N. Kalia, "Effect of controlled laser microporation on drug transport kinetics into and across the skin," J. Control. Release **146**(1), 31–36 (2010).
7. I. A. Aljuffali, C.-H. Lin, and J.-Y. Fang, "Skin ablation by physical techniques for enhancing dermal/transdermal drug delivery," J. Drug Deliv. Sci. Technol. **24**(3), 277–287 (2014).
8. G. S. Terentyuk, E. A. Genina, A. N. Bashkatov, M. V. Ryzhova, N. A. Tsyganova, D. S. Chumakov, B. N. Khlebtsov, A. A. Sazonov, L. E. Dolotov, V. V. Tuchin, N. G. Khlebtsov, and O. A. Inozemtseva, "Use of fractional laser microablation and ultrasound to facilitate the delivery of gold nanoparticles into skin in vivo," Quantum Electron. **42**(6), 471–477 (2012).
9. A. V. Belikov, A. V. Skrypnik, K. V. Shatilova, and V. V. Tuchin, "Multi-beam laser-induced hydrodynamic shock waves used for delivery of microparticles and liquids in skin," Lasers Surg. Med. **47**(9), 723–736 (2015).
10. E. A. Genina, L. E. Dolotov, A. N. Bashkatov, G. S. Terentyuk, G. N. Maslyakova, E. A. Zubkina, V. V. Tuchin, I. V. Yaroslavsky, and G. B. Altshuler, "Fractional laser microablation of skin aimed at enhancing its permeability for nanoparticles," Quantum Electron. **41**(5), 396–401 (2011).
11. E. A. Genina, A. N. Bashkatov, L. E. Dolotov, G. N. Maslyakova, V. I. Kochubey, I. V. Yaroslavsky, G. B. Altshuler, and V. V. Tuchin, "Transcutaneous delivery of micro- and nanoparticles with laser microporation," J. Biomed. Opt. **18**(11), 111406 (2013).
12. H.-J. Laubach, Z. Tannous, R. R. Anderson, and D. Manstein, "Skin responses to fractional photothermolysis," Lasers Surg. Med. **38**(2), 142–149 (2006).
13. J. Klesing, A. Wiehe, B. Gitter, S. Gräfe, and M. Epple, "Positively charged calcium phosphate/polymer

#256837 Received 4 Jan 2016; revised 14 Apr 2016; accepted 18 Apr 2016; published 3 May 2016

nanoparticles for photodynamic therapy," J. Mater. Sci. Mater. Med. **21**(3), 887–892 (2010).
14. J. Qian, D. Wang, F. Cai, Q. Zhan, Y. Wang, and S. He, "Photosensitizer encapsulated organically modified silica nanoparticles for direct two-photon photodynamic therapy and in vivo functional imaging," Biomaterials **33**(19), 4851–4860 (2012).
15. Yu. I. Svenskaya, N. A. Navolokin, A. B. Bucharskaya, G. S. Terentyuk, A. O. Kuz'mina, M. M. Burashnikova, G. N. Maslyakova, E. A. Lukyanets, and D. A. Gorin, "Calcium carbonate microparticles containing a photosensitizer Photosens: preparation, ultrasound stimulated dye release, and in vivo application," Nanotechnol. Russ. **9**(7–8), 398–409 (2014).
16. International Guiding Principles for Biomedical Research Involving Animals, CIOMS&ICLAS, http://www.cioms.ch/index.php/12-newsflash/227-cioms-and-iclas-release-the-new-international-guiding-principles-for-biomedical-researchinvolving-animals.
17. Y. Cai, M. Xu, M. Yuan, Z. Liu, and W. Yuan, "Developments in human growth hormone preparations: sustained-release, prolonged half-life, novel injection devices, and alternative delivery routes," Int. J. Nanomedicine **9**, 3527–3538 (2014).
18. J. W. Lee, S. O. Choi, E. I. Felner, and M. R. Prausnitz, "Dissolving microneedle patch for transdermal delivery of human growth hormone," Small **7**(4), 531–539 (2011).
19. F. Chen, P. Huang, C. Qi, B.-Q. Lu, X.-Y. Zhao, C. Li, J. Wu, D.-X. Cui, and Y.-J. Zhu, "Multifunctional biodegradable mesoporous microspheres of Eu^{3+}-doped amorphous calcium phosphate: microwave-assisted preparation, pH-sensitive drug release, and bioimaging application," J. Mater. Chem. B Mater. Biol. Med. **2**(41), 7132–7140 (2014).
20. A. Sergeeva, R. Sergeev, E. Lengert, A. Zakharevich, B. Parakhonskiy, D. Gorin, S. Sergeev, and D. Volodkin, "Composite magnetite and protein containing CaCO3 crystals. External manipulation and vaterite → calcite recrystallization-mediated release performance," ACS Appl. Mater. Interfaces **7**(38), 21315–21325 (2015).
21. G. Oni, S. A. Brown, and J. M. Kenkel, "Can fractional lasers enhance transdermal absorption of topical lidocaine in an in vivo animal model?" Lasers Surg. Med. **44**(2), 168–174 (2012).
22. B. D. Zelickson, S. E. Walgrave, M. Y. H. Al-Arashi, G. B. Altshuler, I. V. Yaroslavsky, J. J. Childs, R. H. Cohen, A. V. Erofeev, E. F. Depina, M. Z. Smirnov, D. A. Kist, and D. R. Tabatadze, "Semi-Automated method of analysis of horizontal histological sections of skin for objective evaluation of fractional devices," Lasers Surg. Med. **41**(9), 634–642 (2009).
23. C.-H. Lin, I. A. Aljuffali, and J.-Y. Fang, "Lasers as an approach for promoting drug delivery via skin," Expert Opin. Drug Deliv. **11**(4), 599–614 (2014).
24. P. Matteini, F. Ratto, F. Rossi, and R. Pini, "Laser-activated nano-biomaterials for tissue repair and controller drug release," Quantum Electron. **44**(7), 675–682 (2014).
25. H.-J. Jang, E. Hur, Y. Kim, S.-H. Lee, N. G. Kang, and J. J. Yoh, "Laser-induced microjet injection into preablated skin for more effective transdermal drug delivery," J. Biomed. Opt. **19**(11), 118002 (2014).
26. H.-C. Chang, Y.-H. Lin, and K.-C. Huang, "Accurate laser skin perforation technique aimed at promoting bleeding and reducing pain," J. Innov. Opt. Health Sci. **8**(6), 1550029 (2015).

1. Introduction

The importance of drug delivery and creation a long-term depot in skin for topically applied compounds has been demonstrated [1,2]. The stratum corneum (10-20 μm) and underlying living epidermis (75-150 μm) represent a barrier, which makes the delivery of medicaments into dermis a rather problematic [2]. It is possible to use micro- and nanoparticles as drug carriers for efficient localized delivery and storage of topically applied substances into skin appendages [3]. However, in dependence on anatomical sites and individuals, dimensions and density of these natural pathways vary widely [4]. Besides, particles with a diameter more than 100 nm cannot penetrate from the appendages into surrounding tissue [5].

Various strategies including complex physical enhancement methods have been developed for effective transcutaneous delivery of micro- and nanoparticles, including artificial channels produced laser microporation [6–9]. Creating artificial channels by means of FLMA promotes deeper and better targeted delivery of particles in tissue. By changing the parameters of laser beam, one can achieve different depths and shapes of the channels in skin [6–11], inducing e.g. pores with depth from 20 to 500 μm and diameters from 150 to 200 μm [6–8] or creating horizontal cuts with the depth from 150 to 300 μm [10] and channels with the depth up to 2 mm (to demonstrate the possibilities of the technique) [9]. Minimal invasiveness of FLMA and minimal risk of infection in comparison with surface ablation or mechanical treatments are provided by the small area of skin surface damage. The results of observations have shown the complete epidermal healing occurring within a week [11,12].

Different containers have been suggested as carriers of drugs and photosensitizers, including calcium phosphate [13] and silica nanoparticles [14]. To solve the drug localization problem, the use of calcium carbonate microparticles ($CaCO_3$) in the vaterite polymorphic

#256837 Received 4 Jan 2016; revised 14 Apr 2016; accepted 18 Apr 2016; published 3 May 2016

form was earlier suggested in [15]. They showed a number of advantages such as porous structure, mild decomposition conditions, biocompatibility, preparation simplicity, and low production cost.

In this article, we are presenting results on delivery of $CaCO_3$ containers filled up by Fe_3O_4 nanoparticles into the rat skin *in vivo* using a newly designed FLMA-protocol providing increased particle delivery depth aiming to develop a method of long-term depot formation within the dermis.

2. Materials and methods

Animal experiments were performed in accordance with the International Guiding principles for Biomedical Research Involving Animals [16]. A total of 6 male outbred albino rats weighing 200 ± 20 g were used. The treated areas were chosen on a dorsum and were divided into three sites 10 × 10 mm. Prior to the treatment, the rats were anaesthetized with Zoletil 50 (Virbac, France) in dose of 0.05 mg/kg. Hair from the areas was removed with a depilatory cream. Before commencing the experiment the skin sites were disinfected with 40% ethanol. Both the first and the second sites were microporated with FLMA (Fig. 1). The third one remained intact. Water suspension of $CaCO_3$ microcontainers (4.0 ± 0.8 μm) containing Fe_3O_4 nanoparticles (14 ± 5 nm) was prepared. The suspension with concentration 1 mg/mL was applied on the surface of the first and the third sites. The solution of chlorhexidine was added to the suspension in the proportion 2:3 to prevent the infection of the target skin areas. For delivery of the particles mechanical massage for 5 min was used. Then, the particles were removed from the skin surface by distilled water.

FLMA of skin was provided by a system based on a pulsed Er:YAG laser (Palomar Medical Technologies Inc., Burlington, MA, USA) with the following parameters: the wavelength 2940 nm, the pulse energy 3.0 J, the pulse duration 15 ms, the number of pulses 3 with the repetition frequency of 1 Hz. Each laser pulse included a series of 3 subpulses with duration 135 μs. The laser beam was split into 169 micro-beams using an array of micro-lenslets. Thus, 169 vertical cone-shaped microchannels were created in the skin in the site with the dimensions of 6 × 6 mm^2. Such mode of laser irradiation allowed us to increase the depth of laser produced channels bigger than 400 μm without additional transverse injury of the skin tissue.

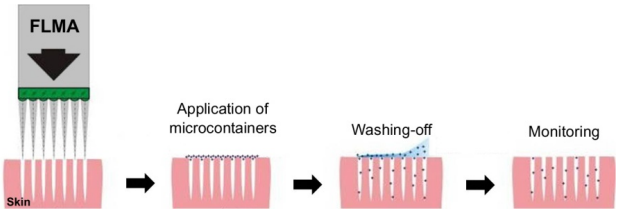

Fig. 1. Sequence of activities at the transcutaneous delivery of $CaCO_3$ microcontainers: fractional laser microablation and microchannel creation in skin; application of suspension of the microcontainers and massage for their administering to the channels; washing-off the microcontainers from skin surface; and monitoring of microcontainer delivery.

The microcontainer suspension was administered into skin of all experimental animals in the same day. The skin was analyzed before the treatment and immediately after the FLMA and particle administration, that is 24 h, 2 days, 3 days, 4 days, and 7 days after the treatment. Optical coherence tomography (OCT) and light microscopy of histological specimens were used for monitoring of the treated skin sites. The animals were withdrawn from the experiment one by one: the first rat immediately after the particle administration and the following rats on the days of the monitoring.

Visualization of microchannels filled with the suspension of the microcontainers was implemented using a commercially available OCT system (OCP930SR, Thorlabs, USA) with the central wavelength 930 ± 50 nm. The axial and lateral resolutions of the light source in air were 6.2 μm and 9.6 μm, respectively.

#256837 Received 4 Jan 2016; revised 14 Apr 2016; accepted 18 Apr 2016; published 3 May 2016

Afterwards, biopsies were taken from the skin sites previously analyzed by OCT. The histological sections were prepared using standard procedure. The paraffined sections of 6 to 8 μm thickness were stained with haematoxylin and eosin. Histological samples were estimated with medical microimager LOMO μ103 (LOMO, Russia).

3. Results and discussion

Figure 2 shows the representative OCT-images of rat skin before and after FLMA alone (a-d) and FLMA and embedding of $CaCO_3$ microcontainers loaded with Fe_3O_4 (e-h) obtained during a week. The depth of the OCT probing is 300-350 μm. Figure 3 shows the microscopic images of longitudinal histological sections obtained from the same sites, which are presented in Fig. 2(e)-2(h).

Figures 2(a), 2(e) and 3(a) correspond to intact rat skin. In Fig. 3(a) it is well seen some hair follicles (the largest of them are marked by arrows). Figure 2(b) shows the skin 24 hours after FLMA. We can see two microchannels edged by a layer of coagulated tissue. Coagulated skin is less scattering, therefore, in OCT-image is seen darker than surrounded tissue.

Figures 2(f) and 3(b) are also obtained 24 hours after FLMA but they differ by the embedding of the particle suspension. In the OCT-image the particles filling the channels (marked by rectangles) have a very good contrast because they have higher refraction index than surrounding tissue. Besides, they have a high reflectance (they are seen as white) therefore, the OCT probing depth decreases significantly in the areas of the $CaCO_3$ localization.

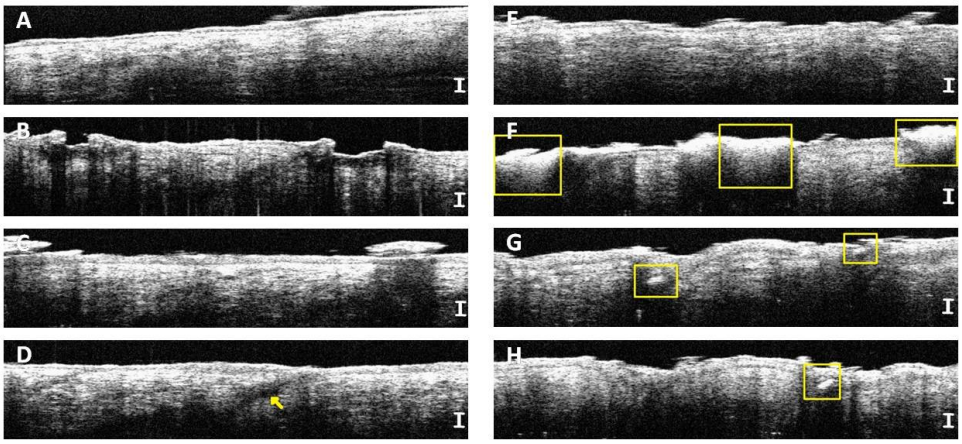

Fig. 2. OCT-images of intact rat skin (A,E); 24 hours (B,F); four days (C,G); and seven days (D,H) after FLMA alone (A-D) and FLMA with embedding of microcontainers $CaCO_3$ loaded with Fe_3O_4 (E-H). Arrow shows the image of a hair follicle. Rectangles show the sites of channels filled with the microcontainers. Bars correspond to 100 μm.

After the staining with haematoxylin and eosin, $CaCO_3$ microcontainers are not visualized, however loading with Fe_3O_4 allows staining the particles in a histological image: they are well visualized as bright blue spheres. Such content of the containers has been chosen specifically to improve their visualization. Histological section in Fig. 3(b) shows the profile of the channel with microcontainers localized along the walls of the channel. The channel is edged with a layer of coagulated tissue (it has darker stain), which is thick enough near skin surface (100 ± 22 μm) and becomes thinner with the depth, up to 30 ± 13 μm at the bottom of the channel. In Fig. 3(b) a follicle surrounded by a sebaceous gland is marked by an arrow. It is well seen that the particles have not filled up a follicle and sebaceous gland. The large size of the containers has not allowed them to penetrate into the follicles.

Figures 2(c), 2(g) and 3(c) show the state of tissue four days after the treatment. In Fig. 2(c) we can see two totally healed channels with scabs on the surface of the skin. Scabs form

#256837 Received 4 Jan 2016; revised 14 Apr 2016; accepted 18 Apr 2016; published 3 May 2016

within the sites of ablation and include necrotic tissue. In Fig. 2(g) in the place of the channels, two local bright areas are well visualized. We suppose that these areas correspond to the localization of the particles, which remained inside tissue after the healing of the channels. Figure 3(c) shows that the particles indeed are inside the dermis (marked by a rectangle), at that, hair follicles and sebaceous glands are free from the particles. Insertion shows a magnified image (× 774.0) of the area of the skin with the microcontainers. It is well seen that they hold the spherical shape and blue staining. It indicates that release of nanoparticles Fe_3O_4 from the containers has not occurred during four days.

In Fig. 2(d), 2(h) (seven days after the treatment) we cannot denote any differences from intact skin. Apparently, the containers have destroyed and dissolved under action of surroundings. However, Fig. 3(d) shows the stained area under the epidermal layer (marked by a rectangle) on the depth about 150 μm. The containers are not visualized, but the staining indicates that release of the nanoparticles have taken place.

The microcontainers $CaCO_3$ were earlier shown [15] to be dissolved in buffer solutions (pH = 5) during 5 min, that was followed by the encapsulated dye releasing. In the cited work the microcontainers were suspended in solutions, therefore the dissolution of the particles could be fast enough. In the surrounding tissue, where the interaction of the containers with interstitial fluid is limited, the containers remained during four days without significant damage, and the nanoparticles were kept inside the containers. Also in Ref [15] it was shown that low-frequency ultrasound enhanced drug release from the $CaCO_3$ microcontainers that could be helpful for controlled drug release in many practical medical tasks.

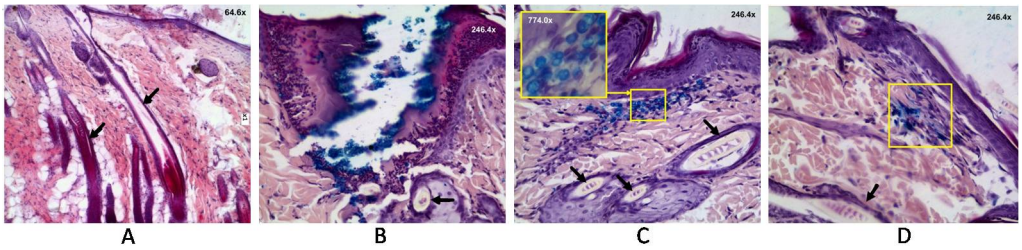

Fig. 3. Images of histological sections of intact rat skin (A); 24 hours (B); four days (C); and seven days (D) after FLMA and embedding of microcontainers $CaCO_3$ loaded with Fe_3O_4. Arrows show the images of hair follicles. Rectangles show the sites with microcontainers. Magnified image is shown in the upper corner for (C).

Figure 4 shows the histological section of intact skin 24 hours after application of $CaCO_3$-Fe_3O_4 suspension and massage for 5 min. The microcontainers are well seen to localize in SC of epidermis only (marked by a rectangle). On the whole, the particle suspension has visualized in the hollows on the skin surface including the openings of hair follicles. But we have not observed the particles inside the follicles or living epidermal tissue.

Thus, the microcontainers are large enough for penetration in depth of follicles as well as inside epidermis excluding the surface layer of SC under action of massage alone. Potentially, US-treatment can facilitate deeper penetration of the particles along the follicles. However, the use of US is not suitable in this case because it can enhance the release of the contents of the microcontainers.

Targeted delivery of biodegradable microspheres as well as other carriers providing sustained release of their contents are actual tasks for many medical applications and are discussed widely in literature [2,13,15,17–20]. However, penetration of carriers through skin epidermal barrier remains a significant problem. The microneedle array is a well developed method for transdermal delivery [2,17].

FLMA can promote penetration of the particles and drugs into dermis to the depth defined by parameters of laser system [7–11,21–23]. Thus, in Ref [21] authors used the laser fluence 125 J/cm^2 to induce areas with ablative depth up to 500 μm within the area of ablation of 1cm^2. The developed FLMA-protocol has allowed us to provide a comparable ablative depth (~400 μm) with the significantly smaller (~0.1 cm^2) area in rat skin *in vivo* at the

#256837 Received 4 Jan 2016; revised 14 Apr 2016; accepted 18 Apr 2016; published 3 May 2016

approximately similar laser fluence ~100 J/cm^2 that promotes much better skin healing. In the papers [8,11] the FLMA with pulse energy 3 J was used for creation of channels with the depth 200-230 μm. At the same energy 3 J or 18 mJ/microbeam we have achieved almost double increasing of the depth. In works [9] and [22] authors have demonstrated a possibility of FLMA to create the channels with the depth >2 mm in vitro by multiple repeating the laser pulses in one case with energy 60 and in another case 24 mJ/microbeam. The comparison of these data with our results is difficult because of the significant differences of laser irradiation parameters. Thermal injury of channel walls was not evaluated in the cited works exept Ref [22]. In this work it was found that the depth of thermal injury is minimal at the bottom of the channels and is of 15-25 μm that is well fit to our data (30 ± 13 μm) accounting for differences in skin type and conditions. In Ref [22] *ex vivo* pig skin was studied as we punctured rat skin *in vivo*.

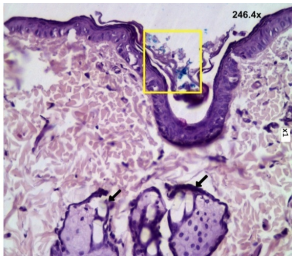

Fig. 4. Image of histological section of intact skin 24 hours after embedding of the microcontainers $CaCO_3$ loaded with Fe_3O_4. Arrows show the images of hair follicles with sebaceous glands. Rectangle shows the site with microcontainers. Magnified image is shown in the upper corner.

Biodegradability of microcarriers is important advantage [18–20]. Time stability of $CaCO_3$ microcontainers containing Fe_3O_4 nanoparticles with and without polyelectrolyte shell in water was studied in [20]. Recently, medical formulation was encapsulated in 600 μm long microneedles composed of carboxymethylcellulose and trehalose, which could be dissolved in body fluid [18]. Authors of Ref [19] have shown that the dissolution percentage of Ca^{2+} ions increases with decreasing of pH of buffer solutions. Thus, pH of surrounding tissue can be the control parameter for drug release from calcium microspheres. In Ref [24] thermosensitive micelles with laser-stimulated drug release were developed.

Described microablation drug delivery technology has good perspectives for clinical applications also due to recent design of portable and efficient erbium laser devices for tissue microporation [25,26].

4. Conclusion

This study shows that the use of fractional laser microablation with the Er:YAG laser allowed efficient target delivery of $CaCO_3$ microcontainers loaded with Fe_3O_4 into dermis. At the pulse energy 3 J and three successive pulses, the lattice of microscopic channels was created in the tissue that promoted particle penetration up to 400 μm deep into the dermis. It is twice deeper than has been achieved in our earlier works (200-230 μm) at one pulse with the same value of energy. The minimal additional injury of the skin gives a good opportunity to use this technology to create a depot for encapsulated drugs that exists inside the tissue for longer time. After seven days we observed microcontainer dissolution and the release of Fe_3O_4 nanoparticles into the dermis. The reported results can be used for further development of methods for controlled drug release and particle delivery in any soft and hard tissue.

Acknowledgments

The research was supported by the Government of the RF (grant 14.Z50.31.0004 to support scientific research projects implemented under the supervision of leading scientists).

#256837 Received 4 Jan 2016; revised 14 Apr 2016; accepted 18 Apr 2016; published 3 May 2016